Performance Evaluation 166 (2024) 102447

Contents lists available at ScienceDirect

Performance Evaluation

journal homepage: www.elsevier.com/locate/peva

An experimental study on beamforming architecture and full-duplex wireless across two operational outdoor massive MIMO networks

Hadi Hosseini [a], Ahmed Almutairi [a], Syed Muhammad Hashir [b], Ehsan Aryafar [a,*], Joseph Camp [b]

[a] Computer Science Department, Portland State University, Portland, OR, USA
[b] Department of Electrical and Computer Engineering, Southern Methodist University, Dallas, TX, USA

ARTICLE INFO

Keywords:
Full-duplex
Massive MIMO
Fully digital radios
Hybrid beamforming

ABSTRACT

Full-duplex (FD) wireless communication refers to a communication system in which both ends of a wireless link transmit and receive data simultaneously in the same frequency band. One of the major challenges of FD communication is self-interference (SI), which refers to the interference caused by transmitting elements of a radio to its own receiving elements. Fully digital beamforming is a technique used to conduct beamforming and has been recently repurposed to also reduce SI. However, the cost of fully digital systems dramatically increases with the number of antennas, as each antenna requires an independent Tx-Rx RF chain. Hybrid beamforming systems use a much smaller number of RF chains to feed the same number of antennas, and hence can significantly reduce the deployment cost. In this paper, we aim to quantify the performance gap between these two radio architectures in terms of SI cancellation and system capacity in FD multi-user Multiple Input Multiple Output (MIMO) setups. We first obtained over-the-air channel measurement data on two outdoor massive MIMO deployments over the course of three months. We next study SoftNull and M-HBFD as two state-of-the-art transmit (Tx) beamforming based FD systems, and introduce two new joint transmit-receive (Tx-Rx) beamforming based FD systems named TR-FD^2 and TR-HBFD for fully digital and hybrid radio architectures, respectively. We show that the hybrid beamforming systems can achieve 80%–99% of the fully digital systems capacity, depending on the number of users. Our results show that it is possible to get many benefits associated with fully digital massive MIMO systems with a hybrid beamforming architecture at a fraction of the cost.

1. Introduction

Global mobile data traffic is estimated by ITU (International Telecommunication Union) to grow at an annual rate of around 55 percent from 2020 to 2030 to reach 607 exabytes (EB) in 2025 and 5016 EB in 2030 [1]. Full-Duplex (FD) transmission and massive MIMO (mMIMO) are two candidate technologies to help operators meet this massive traffic demand. Existing wireless networks operate in half-duplex (HD) mode, which means simultaneous transmission and reception happen on two separate frequency bands. With FD, simultaneous transmission and reception can happen on the same frequency band. The main challenge in FD communication is to overcome the self-interference (SI) problem resulting from strong in-band leakage from the transmitter to the receiver on the same device. Initial work on FD focused on radio designs with a small number of antennas [2–10].

* Corresponding author.
E-mail addresses: hadi3@pdx.edu (H. Hosseini), almut8@pdx.edu (A. Almutairi), hashirs@mail.smu.edu (S.M. Hashir), earyafar@pdx.edu (E. Aryafar), camp@lyle.smu.edu (J. Camp).

https://doi.org/10.1016/j.peva.2024.102447

Available online 27 September 2024

On a parallel front, many antenna (e.g., mMIMO) base stations (BSs) have emerged as a key technology to improve the performance and reliability of cellular networks, resulting in a better user experience. With more antennas, BSs can cover a larger area, and support more users simultaneously enabling faster and more reliable data transfer. [11] However, the maximum number of users a BS can accommodate concurrently is constrained by the number of radio frequency (RF) chains available. Despite this, communicating with the maximum allowable number of users may not always be the most efficient approach, especially in systems with numerous antennas, where the ratio of BS antennas to total users antennas is high. Thus, in many practical mMIMO systems, the ratio of the number of antennas to the number of actual users served is much smaller than one [12–14]. The high number of antennas dramatically increases the complexity of original FD architectures. However, it also introduces a new degree of freedom to combat SI. For example, beamforming (which is traditionally used to form beams towards intended users) can now be repurposed to also reduce SI [9,15].

Our goal in this paper is to quantify the gap between two types of beamforming systems, fully digital and hybrid, in terms of SI and capacity over measured outdoor mMIMO channels. In conventional fully digital beamforming, each antenna element has a dedicated radio frequency (RF) chain, which substantially increases the cost for mMIMO systems. Analog beamforming, which uses phase shifters to connect all antennas to a single RF chain, is the simplest way to overcome hardware costs, but it only supports single-user and single-stream communication, resulting in low spectral efficiency. To balance system performance and hardware complexity, hybrid (analog-digital) beamforming has been introduced [16]. Here, the analog beamforming uses phase shifter networks and several antennas can be connected to one RF chain, which reduces the number of required RF chains compared to the number of antennas. As a result, this scheme is cost-effective and consumes less power [17–20]. The digital beamforming, on the other hand, can be carried out at each RF chain at the baseband, enabling the hybrid beamforming to support multi-user and multi-stream communications [15,21–24].

Fig. 1 illustrates the architecture of the two beamforming schemes. In fully digital architecture, the transmit array has precise control over both the amplitude and phase of the signal at each antenna and more flexibility in beamforming. In hybrid beamforming, one RF chain is connected to multiple antennas through phase shifters, which adjust the phase of the signal at each antenna, but the amplitude of the signal is similar among all antennas connected to the same RF chain. Further, hybrid beamforming is often implemented with discrete quantized phase shifters, which limits resolution in terms of the possible phase values they can apply to the signal. For example, for 2 bits phase shifter network the phase of the signal for each antenna can be selected from four possible values: $0°, 90°, 180°$, and $270°$.

In this paper, we explore the performance trade-offs between hybrid and fully digital architectures for FD over outdoor mMIMO BSs. We use real-world channel measurements obtained from two NSF funded platforms: POWDER [25] in Salt Lake City (Utah) and RENEW [26] in Houston (Texas). Both are publicly available, fully programmable, and open-source mMIMO platforms. We consider scenarios involving both single-user and multi-user MIMO communication. We focus on how the performance changes as the number of users increases. The main contributions of our study are summarized as follows:

- **Measurements:** We collected numerous channel measurements from two outdoor real-world platforms in three different (Internal, Downlink (DL), Uplink (UL)) scenarios. Our measurement campaign lasted about three months.
- **Implementation:** We implemented four SI cancellations algorithms: (i) SoftNull [15], which is the state-of-the-art fully digital candidate, and only uses transmit (Tx) beamforming to reduce SI; (ii) M-HBFD, which we introduced in our previous works [27,28] for hybrid setups. This schemes also uses only transmit (Tx) beamforming to reduce SI and enable FD wireless; (iii) TR-FD^2, which is our newly proposed fully digital adaptation of SoftNull to accommodate joint Tx and Rx beamforming, and (iv) TR-HBFD, which is our newly proposed adaptation of M-HBFD to accommodate joint Tx and Rx beamforming for hybrid radio architectures.
- **Public Release:** We have released our code on the project website [29], so that other researchers in the community can build on our work.
- **Performance Evaluation:** We show that with only 5 bits of phase quantization, the hybrid architectures achieve 80%–99% of the corresponding fully-digital architecture capacity, have 2%–30% more SI, and result in 29–35 times increase in per RF chain capacity. We also show that the gap in performance between fully digital and hybrid beamforming in terms of SI cancellation and overall system capacity shrinks, when joint transmit and receive beamforming is employed.

The rest of this paper is organized as follows. We discuss the related work in Section 2. Section 3 describes the FD algorithms studied in this paper. We discuss our measurement campaign in Section 4. Section 5 presents our performance evaluation results. Finally, we conclude the paper in Section 6.

2. Related work

In this section, we discuss the related work on FD designs for fully digital and hybrid mMIMO systems.

Fully Digital Radio Full-Duplex. Fully digital architectures are generally preferred over hybrid architectures for sophisticated many-antenna BSs aiming for full-duplex communication due to their ability to individually control the output of each antenna element in terms of both amplitude and phase [15,23,24]. SoftNull, a prominent fully digital full-duplex (FD) algorithm, effectively reduces SI while maintaining a desired number of antennas for the beamforming purposes. Instead of simply nullifying the antennas contributing most to SI, SoftNull employs a singular value decomposition of the self-interference matrix between all transmit and receive antennas. It then zeroes out the highest correlated vectors. For example, if a higher-level application requires beamforming with six antennas from a transmit array of nine antennas, SoftNull nullifies the three linear combinations of transmit antennas

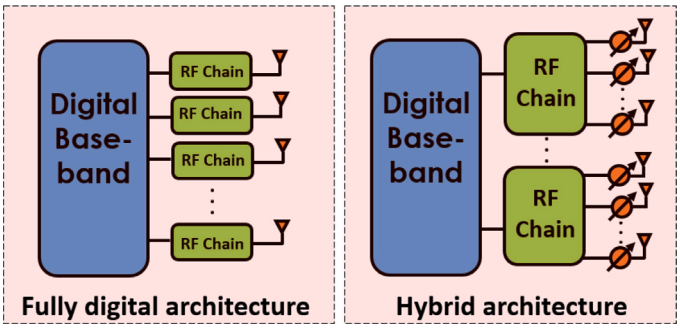

Fig. 1. Illustration of fully digital and hybrid architectures. In fully digital (left), the precise amplitude and phase of signal on each antenna element can by fully controlled. In hybrid (right), the same signal is fed to all antennas connected to the same RF chain, however, the phase of each signal is adjusted by a phase shifter.

contributing most to SI, allowing the remaining six antennas to be utilized for beamforming as desired. Notably, SoftNull primarily focuses on transmit beamforming only. Other studies [21,24,30] have explored the advantages of joint transmit and receive beamforming in fully digital mMIMO systems. In [21], authors propose a phased array architecture employing joint transmit and receive beamforming to mitigate SI and enhance spectral efficiency. JointNull [24] optimizes partial analog cancellation and transmit beamforming simultaneously. It achieves this by assigning each antenna one of three roles: full-duplex, half-duplex receive, and half-duplex transmit antennas. Subsequently, it designs a transmit precoder to suppress SI on the receive antennas.

Hybrid Radio Full-Duplex. Hybrid architectures have the potential to achieve significant reductions in SI without the need to increase the number of RF chains. In PAFD [9], the authors discuss the trade-off between beamforming gain and SI reduction by adjusting the phase shifters on each antenna element. Particularly in scenarios where the SI at each receive antenna is highly correlated, such as in linear arrays, PAFD demonstrates effective SI reduction and beamforming gain. Several other works [31–37] have investigated SI cancellation in hybrid beamforming systems, albeit primarily focusing on mmWave or smaller antenna systems. In our prior work [27], we explored the performance tradeoffs between fully digital and hybrid beamforming systems by introducing a hybrid SI cancellation algorithm named M-HBFD and evaluating its efficacy over measured channels. However, the measurement data was obtained from an 18-antenna indoor testbed with users situated 1–2 m away from the BS. Expanding upon our previous study, in [28], we conducted experiments using data from POWDER mMIMO testbed, featuring a significantly higher number of BS antennas (60–96), in planned outdoor deployments, and with typical cellular users and BS configurations, including distances and heights. Both of our prior studies utilized transmit (Tx) beamforming only to mitigate SI and enable full-duplex (FD) communication. In this paper, we extend our investigation by studying joint transmit-receive (Tx-Rx) beamforming, implementing TR-FD[2] for fully digital architecture and TR-HBFD for hybrid architecture, utilizing real-world channel measurements obtained from both the POWDER and RENEW mMIMO platforms.

3. Full-Duplex algorithms

In this section, we start by presenting the system model. Subsequently, we describe the essential elements of SoftNull and M-HBFD, both of which utilize transmit-only SI cancellation techniques[1]. Finally, we discuss TR-FD[2] and TR-HBFD, which exploit joint transmit-receive SI cancellation mechanisms.

3.1. System model

We assume a BS with M_{Tx} transmit and M_{Rx} receive antennas[2]. The BS simultaneously transmits to K_d DL users and receives data from K_u UL users. A transmit array can be divided into N_{Tx} subarrays, where N_{Tx} can be any whole factor of the rows in the Tx array. For example, let $M_{Tx} = 32$, then if $N_{Tx} = 2$, the Tx array is divided into two subsets each with 16 antennas, which by concatenation the original array can be restored (Fig. 2).

The self-interference channel matrix is denoted by $\mathbf{H}_{self} \in \mathbb{C}^{M_{Rx} \times M_{Tx}}$. Similarly, the SI channel matrix between a transmit subarray i and the receive array is denoted by $\mathbf{H}_{sub_{i,all}} \in \mathbb{C}^{M_{Rx} \times M_{Tx}/N_{Tx}}$, the UL channel matrix is denoted by $\mathbf{H}_u \in \mathbb{C}^{M_{Rx} \times k_u}$, the DL channel matrix is denoted by $\mathbf{H}_d \in \mathbb{C}^{k_d \times M_{Tx}}$, and the channel matrix between a transmit subarray i and the DL users is denoted by $\mathbf{H}_{d_i} \in \mathbb{C}^{k_d \times M_{Tx}/N_{Tx}}$. Then, the signal received by the Rx array can be written as:

$$\mathbf{y}_u = \mathbf{H}_u \mathbf{x}_u + \mathbf{H}_{self} \mathbf{x}_d + \mathbf{z}_u \tag{1}$$

[1] Our focus in this paper is to study the amount of reduction in SI in mMIMO system through beamforming. As a result, there is still residual SI. It is possible to completely remove this SI, e.g., through combination of digital cancellation on top of the proposed methods and use of absorbers to further reduce the coupling between Tx and Rx antennas, but this is beyond the scope of this paper.

[2] Unless otherwise stated, we equally divide the total available antennas at the BS into transmit and receive antennas.

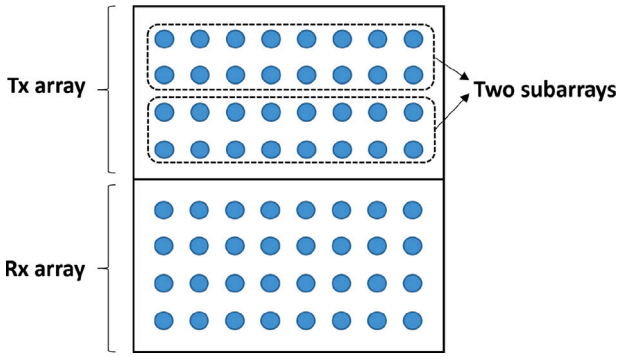

Fig. 2. BS model with $M_{Tx} = 32$, $M_{Rx} = 32$ and $N_{Tx} = 2$.

where $\mathbf{x}_u \in \mathbb{C}^{k_u \times 1}$, $\mathbf{x}_d \in \mathbb{C}^{k_d \times 1}$ are vectors of the transmitted symbols by the UL users and the Tx array respectively, and $\mathbf{z}_u \in \mathbb{C}^{M_{Rx} \times 1}$ captures the noise.

If we ignore the user-to-user interference, DL users will receive the signal below:

$$\mathbf{y}_d = \mathbf{H}_d \mathbf{x}_d + \mathbf{z}_d \tag{2}$$

where $\mathbf{z}_d$ is noise at DL users.

3.2. Tx only SI cancellation

We now present two DL beamforming solutions employed at the BS that not only use beamforming as a means to increase users signal strength, but also to reduce SI. Note that for ease of discussion we assume FD is only enabled at the BS and users operation in HD mode.

SoftNull Components: SoftNull [15] is composed of two main stages. The first stage is the standard MU-MIMO precoder (denoted by $\mathbf{P}_d \in \mathbb{C}^{D_{Tx} \times K_d}$) which precodes signals between D_{Tx} effective antennas and K_d users, and second stage is the self-interference reduction stage with the SoftNull precoder (denoted as $\mathbf{P}_{self} \in \mathbb{C}^{M_{Tx} \times D_{Tx}}$). Effective antennas capture the set of antennas used for DL communication. Now, let $\mathbf{s}_d \in \mathbb{C}^{K_d \times 1}$ denote the vector of symbols that the base station wishes to communicate to each of the K_d DL users. The signal transmitted from the BS antennas is then $\mathbf{x}_d = \mathbf{P}_{self}\mathbf{P}_d\mathbf{s}_d$. $\mathbf{P}_d$ can be selected from standard precoders, such as zero-forcing, and only requires knowledge of the effective DL channel, which is $\mathbf{H}_{Eff_d} = \mathbf{H}_d\mathbf{P}_{self}$, and does not need separate knowledge of the $\mathbf{H}_{self}$ and the physical DL channel. For instance, in zero-forcing beamforming, $\mathbf{P}_d$ is the Moore–Penrose pseudoinverse of the $\mathbf{H}_{Eff_d}$:

$$\mathbf{P}_d = \alpha \mathbf{H}_{Eff_d}(\mathbf{H}_{Eff_d}^H \mathbf{H}_{Eff_d})^{-1} \tag{3}$$

where α is a power constraint coefficient. The SoftNull precoder specifies D_{Tx} effective antennas that have the least interference on the receive array by taking a singular value decomposition (SVD) of the SI matrix between all transmit and receive antennas and sets the other highly correlated $(M_{Tx} - D_{Tx})$ antennas, which play the most role in the self-interference, to zero. The dimensionality of the transmit array reduces to D_{Tx} by nulling (soft nulling) these antennas. $\mathbf{P}_{self}$ is constructed by projecting onto the D_{Tx} left singular vectors of the $\mathbf{H}_{self}$:

$$\mathbf{P}_{self} = [\mathbf{v}^{(M_{Tx}-D_{Tx}+1)}, \mathbf{v}^{(M_{Tx}-D_{Tx}+2)}, \ldots, \mathbf{v}^{M_{Tx}}] \tag{4}$$

where $\mathbf{H}_{self} = \mathbf{U}\mathbf{\Sigma}\mathbf{V}^H$ is the SVD of the $\mathbf{H}_{self}$, and $\mathbf{v}^{(i)}$ is the ith column of $\mathbf{V}$.

M-HBFD: M-HBFD [27] is an adaptation of SoftNull for hybrid beamforming architectures[3]. M-HBFD divides the Tx array into N_{Tx} subarrays and each subarray uses a single RF chain to communicate with a single DL user. For example, in the case of $M_{Tx} = 32$ and $N_{Tx} = 2$, we have two subarrays, each with 16 antennas connected to one RF chain and we have two total RF chains that transmit to two users. SoftNull is calculated separately for each subarray, using the SI matrix $\mathbf{H}_{sub_{i,all}}$, which represents the relationship between subarray i and the receive array. The total number of effective antennas for the transmit array is then divided equally among the subarrays to determine the number of effective antennas used for each subarray's SoftNull calculation. For example, for the above-mentioned scenario, if $D_{Tx} = 20$, then each subarray would use 10 effective antennas for SoftNull calculation, and the

[3] Our prior work [27], compares the performance of M-HBFD against SoftNull in an indoor environment with a small antenna BS, and users which are 1–2 m away from the BS. This work is conducted over two outdoor mMIMO deployments with a much higher number of antennas as well as a planned layout (e.g., BS/user heights, distances) that mimic practical cellular deployments.

singular value decomposition would be taken from $\mathbf{H}_{sub_{i,all}}$. For each Tx subarray we define $\mathbf{P}_{self}^{sub_{Tx}} \in \mathbb{C}^{\frac{M_{Tx}}{N_{Tx}} \times \frac{D_{Tx}}{N_{Tx}}}$ which is constructed by projecting onto the $\frac{D_{Tx}}{N_{Tx}}$ left singular vectors of the $\mathbf{H}_{sub_{i,all}}$:

$$\mathbf{P}_{self}^{sub_{Tx}} = [\mathbf{v}^{(\frac{M_{Tx}}{N_{Tx}} - \frac{D_{Tx}}{N_{Tx}} + 1)}, \mathbf{v}^{(\frac{M_{Tx}}{N_{Tx}} - \frac{D_{Tx}}{N_{Tx}} + 2)}, \ldots, \mathbf{v}^{\frac{M_{Tx}}{N_{Tx}}}] \tag{5}$$

where $\mathbf{H}_{sub_{i,all}} = \mathbf{U}\mathbf{\Sigma}\mathbf{V}^H$ is the SVD of the $\mathbf{H}_{sub_{i,all}}$, and $\mathbf{v}^{(i)}$ is the ith column of $\mathbf{V}$.

Subsequently the standard precoder is $\mathbf{P}_d \in \mathbb{C}^{\frac{D_{Tx}}{N_{Tx}} \times \frac{K_d}{N_{Tx}}}$, and the vector of symbols is $\mathbf{s}_d \in \mathbb{C}^{\frac{K_d}{N_{Tx}} \times 1}$. The signal transmitted from BS antennas to DL users is then $\mathbf{x}_d = \mathbf{P}_{self}^{sub_{Tx}} \mathbf{P}_d \mathbf{s}_d$. The value of $\mathbf{x}_d$ for each physical antenna is approximated to the closest achievable value, depending on the number of quantization bits in the system's architecture.

3.3. Joint Tx-Rx SI cancellation

We now present two joint transmit and receive beamforming solutions employed at the BS. These solution not only increase DL and UL user signal strength, but also reduce SI.

TR-FD^2: In contrast to SoftNull, which exclusively addresses digital SI cancellation and precoder design in DL communication, TR-FD^2 leverages these processes for both transmit and receive arrays in both DL and UL transmissions, respectively. TR-FD^2 is designed for fully digital radios and unfolds in two distinct steps. Initially, $\mathbf{P}_d$ and $\mathbf{P}_{self}$ are computed in two stages mirroring the SoftNull methodology. The subsequent step operates in reverse mode, focusing on UL transmission. Here, the objective is to formulate the UL precoder (referred to as $\mathbf{P}_u \in \mathbb{C}^{K_u \times D_{Tx}}$) relative to the newly formed SI matrix ($\mathbf{H}_{self}^{new} \in \mathbb{C}^{M_{Rx} \times D_{Tx}}$) derived from the prior step. This new SI channel is defined as $\mathbf{H}_{self}^{new} = \mathbf{H}_{self}\mathbf{P}_{self}$. Note that by working on this new SI channel matrix, we aim to remove the remaining SI from highly correlated Tx antennas that was not removed through Tx beamforming only. The effective UL channel is $\mathbf{H}_{Eff_u} = \mathbf{H}_u{}^T \mathbf{P}_{self}$ and, the signal transmitted from the UL users to BS antennas is $\mathbf{x}_u = \mathbf{s}_u \mathbf{P}_u \mathbf{P}_{self}{}^T$ where $\mathbf{s}_u \in \mathbb{C}^{1 \times K_u}$ is the vector of symbols from K_u UL users, and $\mathbf{P}_u$ is:

$$\mathbf{P}_u = \alpha \mathbf{H}_{Eff_u} (\mathbf{H}_{Eff_u}^H \mathbf{H}_{Eff_u})^{-1}. \tag{6}$$

Initially, $\mathbf{P}_u$ is designed using conventional methods such as zero-forcing. Subsequently, we employ a technique similar to SoftNull's reverse mode for the UL channel, where D_{Tx} effective antennas are specified. This involves conducting a singular value decomposition of $\mathbf{H}_{self}^{new}$ and setting the other highly correlated $(M_{Tx} - D_{Tx})$ antennas to zero.

TR-HBFD: TR-HBFD is an adaptation of TR-FD^2 tailored for hybrid beamforming architecture to design both DL and UL precoders. In the initial stage, TR-HBFD performs identical operations as SoftNull on the Tx array and comes up with $\mathbf{H}_{self}^{new}$. In the subsequent stage, the Rx array is divided into N_{Rx} subarrays. Each subarray employs a single radio frequency (RF) chain to communicate with a single UL user. For instance, if the Rx array consists of 32 antennas ($M_{Rx} = 32$) and $N_{Rx} = 2$, there would be two subarrays, each comprising 16 antennas connected to one RF chain. Consequently, there are two RF chains in the Rx array receiving signals from two UL users. We define $\mathbf{H}_{sub_{all,j}}^{new}$, denoting the relationship between the updated transmit array from the previous stage and the j_{th} subarray in the Rx array. The total number of effective antennas for the Rx array denoted by D_{Rx} is then evenly distributed among the subarrays to determine the number of effective antennas utilized for each subarray. Subsequently, SVD is applied to each $\mathbf{H}_{sub_{all,j}}^{new}$, following the procedure in M-HBFD.

For each Rx subarray $\mathbf{P}_{self}^{sub_{Rx}} \in \mathbb{C}^{\frac{D_{Rx}}{N_{Rx}} \times \frac{M_{Rx}}{N_{Rx}}}$ is constructed by projecting onto the $\frac{D_{Rx}}{N_{Rx}}$ left singular vectors of the $\mathbf{H}_{sub_{all,j}}^{new}$:

$$\mathbf{P}_{self}^{sub_{Rx}} = [\mathbf{v}^{(\frac{M_{Rx}}{N_{Rx}} - \frac{D_{Rx}}{N_{Rx}} + 1)}, \mathbf{v}^{(\frac{M_{Rx}}{N_{Rx}} - \frac{D_{Rx}}{N_{Rx}} + 2)}, \ldots, \mathbf{v}^{\frac{M_{Rx}}{N_{Rx}}}] \tag{7}$$

where $\mathbf{H}_{sub_{all,j}}^{new} = \mathbf{U}\mathbf{\Sigma}\mathbf{V}^H$ is the SVD of the $\mathbf{H}_{sub_{all,j}}^{new}$, and $\mathbf{v}^{(i)}$ is the ith column of $\mathbf{V}$.

Subsequently the standard precoder is $\mathbf{P}_u \in \mathbb{C}^{\frac{K_u}{N_{Rx}} \times \frac{D_{Rx}}{N_{Rx}}}$, and the vector of symbols is $\mathbf{s}_u \in \mathbb{C}^{1 \times \frac{K_u}{N_{Rx}}}$. The signal transmitted from the UL users to BS antennas is then $\mathbf{x}_u = \mathbf{s}_u \mathbf{P}_u \mathbf{P}_{self}^{sub_{Rx}}$. Finally it approximates the value of $\mathbf{x}_u$ for each physical antenna in the Rx array to the nearest achievable value, which depends on the number of quantization bits in the system's architecture.

3.4. Computational complexity of the algorithms

To determine the computational complexity of the introduced algorithms described above, we need to analyze two main stages of each algorithm: the MU-MIMO precoding and the SI reduction stage. The first stage in each algorithm involves calculating the zero-forcing precoder, which consists of matrix multiplication and matrix pseudo-inversion. This suggests a polynomial complexity of at most $O({M_{Tx}}^3)$ for the transmitter-side processing or $O({M_{Rx}}^3)$ in the revers mode for receive beamforming. For the second stage, the dominant complexity comes from performing the SVD which is $O({M_{Tx}}^2 \cdot M_{Rx})$ or $O({M_{Rx}}^2 \cdot M_{Tx})$. Therefore, the total complexity of each algorithm is at most a polynomial of degree three.

4. Data gathering

In this section, we discuss the two mMIMO platforms that we used in this study as well as our measurement campaign and methodology.

Fig. 3. We conducted experiments across two mMIMO networks. Left: University of Utah 64-antenna BS, operating in the CBRS band. The BS is installed on the rooftop of the Merrill Engineering Building. On the same rooftop, there are two standalone 2 × 2 MIMO Iris SDRs that act as UEs. A third site for users is currently under construction. Right: Rice University 96-antenna mMIMO BS. The four users each with 2 × 2 MIMO antennas are deployed inside the stadium.

4.1. Outdoor many antenna platforms

We conducted experiments utilizing two different mMIMO testbeds: University of Utah's POWDER testbed and Rice University's RENEW testbed. Both platforms use Iris software defined radios (SDRs) developed by Skylark wireless, which allowed us to use many similar software modules across the two platforms, from the waveforms created for each antenna all the way up to the application layer. Users conducting experiments on these platforms get their own VLANs on these network, allowing them to backhaul to edge computing sites. Profiles help users package up experiment descriptions, including software, radio firmware, and hardware specifications, so that they can run experiments repeatedly [26]. For the POWDER setup, we utilized the Merrill Engineering Building (MEB) rooftop setup, which consists of one BS with 64 antennas and three user sites. For the RENEW testbed, we conducted our experiments using a BS with 96 antennas (with only 80 antennas fully working) and four users which are located inside the Rice University football stadium. The BS is located at the top corner of the stadium. The two systems use different versions of the IRIS hardware and represent two different urban deployments. Fig. 3 shows a screenshot of the two platforms. A brief detailed description of each setup is as follows:

POWDER: The BS is equipped with 8 Remote Radio Head (RRH) units, each containing four 2 × 2 MIMO Iris SDRs operating in the Citizens Broadband Radio Service (CBRS) band (3540 MHz to 3600 MHz). The three user sites each contain a 2 × 2 MIMO Iris SDR that acts as a user. For our experiments, we focused on the BS and user site number one and user site number two, which are located at a distance of 20.1 m and 35.5 m from the BS, respectively. User site number three is still under construction.

RENEW: The BS is equipped with 8 Remote Radio Head (RRH) units, each containing six 2 × 2 MIMO Iris SDRs operating in the CBRS band (3540 MHz to 3600 MHz). The four users each contain a 2 × 2 MIMO Iris SDR that acts as a user. For our experiments, we used 80 antennas (out of the total 96 antennas) of the BS and all four users. The selection of 80 out of 96 is due to our observation that some antennas at the BS were not working properly.

4.2. Measurement campaign

We conducted three main experiments for each setup. In the first set of experiments, we performed UL measurements by transmitting a pre-defined sequence, such as a Zadoff–Chu sequence, from the user and receiving it at the BS. In the second experiment set, we performed downlink measurements by transmitting a pre-defined sequence from the BS and receiving it at the user. In the third experiment set, we conducted internal measurements, which involved transmitting a pre-defined sequence from one antenna of the BS and receiving it at all other antennas of the BS simultaneously. This was done by iterating over all the BS antennas, with each iteration involving one antenna transmitting and the others receiving. Each experiment set is composed of running experiments at different times (e.g., morning, evening, night) and days to capture channels in a variety of conditions.

To perform an experiment, both POWDER and RENEW setups allow a scheduled remote slot to connect to the servers that are directly connected to the testbeds' hardware (BSs and users). We initially used the open-source code provided by the platform operators and Skylark Wireless [38] to run our experiments. Those setups allow user-defined configurations such as specifying the number of antennas at BS and users, number of frames, number of samples, and frequency. We later further optimized the software for calibration and taking internal channel measurements, among others. The measurement process involves the following steps to ensure accuracy of SI characterization in the presence of external sources of interference:

- Calibration: We ensured antenna calibration before each set of experiments to account for any ambient noise and interference. This helps us distinguish SI from other sources of interference.
- Repeated Measurements: To ensure robustness, we repeated measurements multiple times under various conditions (e.g., morning, evening, night). This helps in mitigating the effects of transient external interference.
- Interference Characterization: We finally characterized the external interference separately and account for it in our SI measurements. This involves measuring the noise floor and any persistent interfering signals independently and subtracting their effect from the SI measurements.

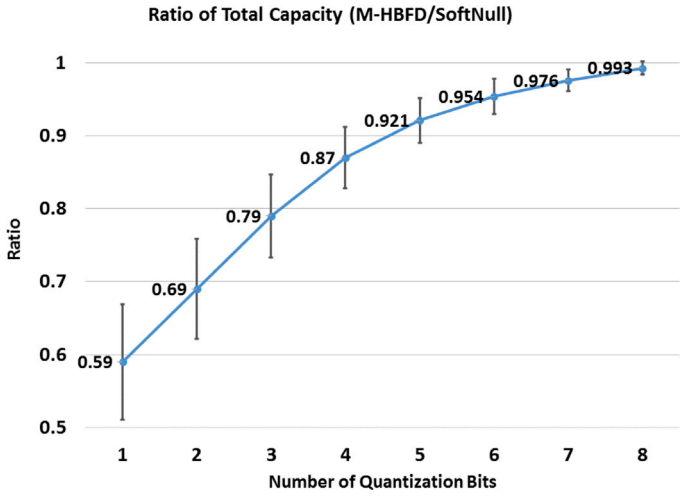

Fig. 4. Capacity ratio with varying quantization bits.

The output of our experiments were captured in the form of IQ samples, which were written into a Hierarchical Data Format 5 (HDF5) file. The dimensions of the HDF5 file were based on the number of frames, cells, pilot slots, BS antennas, and samples in each slot. We finally extract the CSI of the channels for the UL, DL, and between BS antennas using measured IQ samples saved in HDF5 files. We finally process the CSI data offline to obtain our desired performance metrics such as SI, SNR, and wireless capacity.

5. Performance evaluation

In this section, we present the results of our extensive experiments. We first discuss the impact of hybrid radio accuracy (measured in terms of the number of quantization bits) on system capacity. Next, we investigate the tradeoffs between the two systems in terms of SI, capacity, and capacity per RF chain.

5.1. Number of quantization bits

Hybrid beamforming systems use discrete quantized phase shifters, which limits resolution in terms of the possible phase values they can apply to the signal. For example, for 2 bits phase shifter network the phase of the signal for each antenna can be selected from four possible values: $0°, 90°, 180°$, and $270°$. The number of quantization bits is crucial in determining the system's performance. It is necessary to carefully choose an appropriate quantization bit level to optimize the performance and cost of the overall design. We take the following approach to determine an appropriate number of quantization bits. We first compare the ratio of the capacity between M-HBFD and Softnull in terms of the number of quantization bits to find a proper baseline for our comparisons. Fig. 4 shows the ratio of M-HBFD total capacity to SoftNull total capacity for different numbers of quantization bits in the POWDER setup. Each data point is the total capacity of the FD channel for 4 subarrays (communicating with 4 users) and is computed by averaging over 1000 measured channel realizations. Error bars show the confidence interval aournd the estimate.

Since five bits of quantization offers a good capacity approximation (93%) of fully digital architecture, we select this level of quantization as a baseline for other evaluations[4] that will be carried out in the following sections. Table 1 describe basic parameter setting used in our simulations and experiments.

5.2. Self-interference cancellation

Tx Beamfomring Only. Fig. 5 illustrates the impact of the number of subarrays and effective antennas on SI comparing M-HBFD and SoftNull across two testbeds. Each data point is an average of 1000 channel realizations. The x-axis shows the number of transmit subarrays and users. For example in the 1 subarray setup, the BS in hybrid setup would be equipped with only a single RF chain. Further, there is only a single user to be served. Similarly, when the number of subarrays is four, the BS in hybrid setup would have 4 RF chains, and there are 4 users in the network. Table 2 presents the average SI power levels in dBm for various numbers of effective antennas on the POWDER platform. It compares the performance of SoftNull and M-HBFD, providing absolute values for this analysis.

[4] Five bits is a reasonable number in modern systems. Each additional increase in the number of bits can make the overall hardware design much more complex and costly.

Table 1
Basic parameter setting used in simulations and experiments.

Parameter	Value
Number of quantization bits	5
Number of channel realization	1000
Analog SI cancellation	40 dB
Number of BS antennas (POWDER)	64
Number of users (POWDER)	2 (two channels)
Number of BS antennas (RENEW)	80 out of 96
Number of users (RENEW)	4
Operating frequency band	3540 to 3600 MHz
Maximum output power	28 dBm

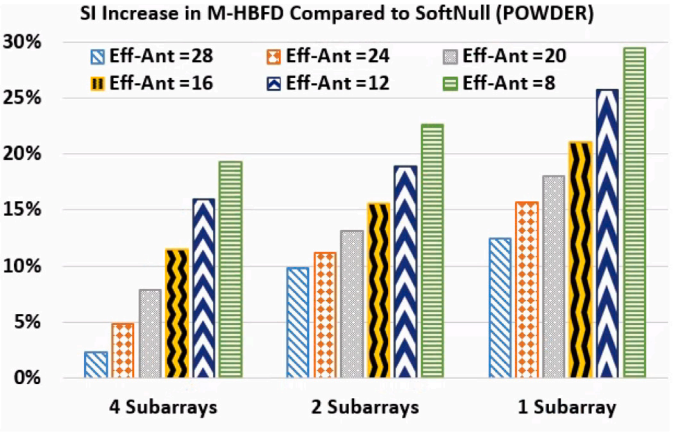

(a) POWDER setup

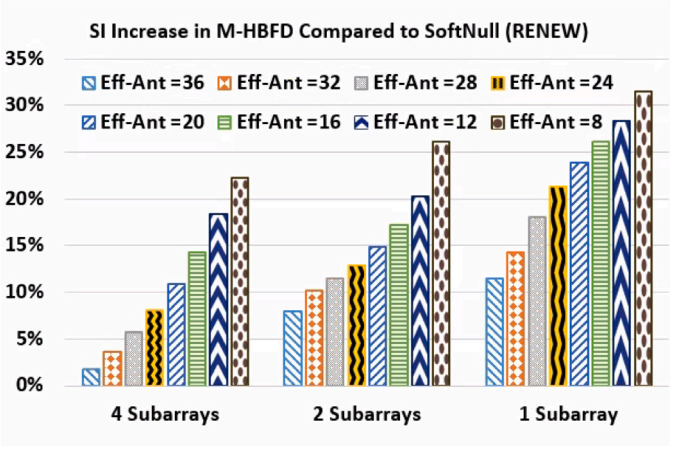

(b) RENEW setup

Fig. 5. POWDER and RENEW SI results for Tx beamforming only. As the number of subarrays (and hence users served) increases, the gap in residual SI between fully digital and hybrid beamforming systems shrinks. This means that in practical mMIMO deployments, there is limited advantage in using fully digital systems in terms of residual SI.

Table 2
Average SI power level (dBm), for different numbers of effective antennas comparing M-HBFD and SoftNull on the POWDER platform.

Algorithm	Eff-Ant = 28	Eff-Ant = 24	Eff-Ant = 20	Eff-Ant = 16	Eff-Ant = 12	Eff-Ant = 8
SoftNull	−36.3	−40.9	−44.2	−49.8	−56.3	−62.3
M-HBFD - 4 Subarrays	−35.4	−38.9	−40.7	−44	−47.3	−50.3
M-HBFD - 2 Subarrays	−32.7	−36.1	−38.3	−42	−45.6	−48.2
M-HBFD - 1 Subarrays	−31.7	−34.4	−36.2	−39.3	−41.7	−43.9

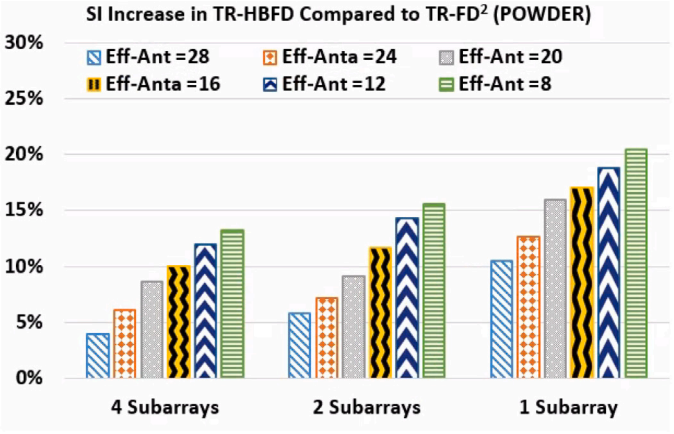

(a) POWDER setup

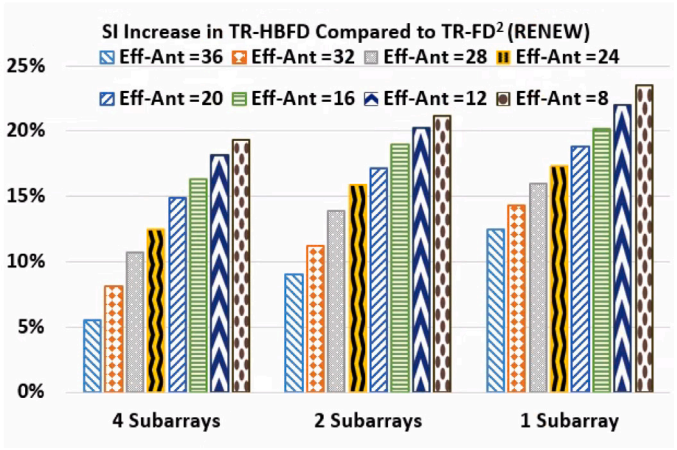

(b) RENEW setup

Fig. 6. POWDER and RENEW SI results for joint Tx and Rx beamforming. There is less residual SI compared to using Tx beamforming only. In other words, the gap in terms of SI cancellation between fully digital and hybrid beamforming systems is even less when joint transmit and receive beamforming is used.

We observe that when M-HBFD is employed, SI is higher when compared to SoftNull, across all scenarios studied. SoftNull additional SI cancellation gain to M-HBFD is 2.4% to 29% on the POWDER setup, and 1.8% to 31% on the RENEW setup. The disparity between the two methods was smaller when using more effective antennas, or when communicating with multiple users concurrently. SoftNull's maximum performance advantage is limited to only about 30% on both setups, indicating that a substantial portion of the SI in the results can be effectively mitigated by both SoftNull and M-HBFD techniques, or may remain unaffected by either method. The inclusion of additional effective antennas reduces the SI cancellation advantage of SoftNull, and depending on the other SI cancellation techniques on the receiver side, the number of effective antennas can be optimally selected. In M-HBFD, as the number of users increases by augmenting the number of subarrays, the discrepancy in SI between the two algorithms decreases. This suggests that if the mMIMO BS communicates with more users simultaneously, hybrid and fully digital beamforming systems would have a very narrow performance gap in terms of overall FD SI.

Joint Tx-Rx Beamforming. Fig. 6 illustrates the impact of the number of subarrays and effective antennas on SI, comparing TR-HBFD and TR-FD^2 across the two testbeds. The additional SI cancellation gain provided by TR-FD^2 over TR-HBFD ranges from 3.9% to 21% on the POWDER setup and from 5.8% to 23.5% on the RENEW setup. In comparison to Tx beamforming alone, the maximum performance advantage of TR-FD^2 is limited to approximately 23.5% on both setups. This suggests that the difference in SI between fully digital and hybrid Tx-Rx beamforming methods is even less pronounced than with Tx beamforming alone. Furthermore, the inclusion of additional effective antennas diminishes the SI cancellation advantage of TR-FD^2, displaying a similar trend to Tx beamforming alone but with a more gradual slope. One plausible explanation for this phenomenon could be the utilization of the new reduced self-interference channel matrix for Rx beamforming resulting from Tx beamforming in the initial stage.

Comparison Between Tx Only and Joint Tx-Rx Beamforming. In the preceding analysis, we compared each hybrid beamforming architecture against its fully digital counterpart. We now turn our attention to comparing the extent of self-interference (SI) reduction between TR-HBFD and M-HBFD. In other words, we aim to quantify the benefit of joint Tx-Rx beamforming against Tx

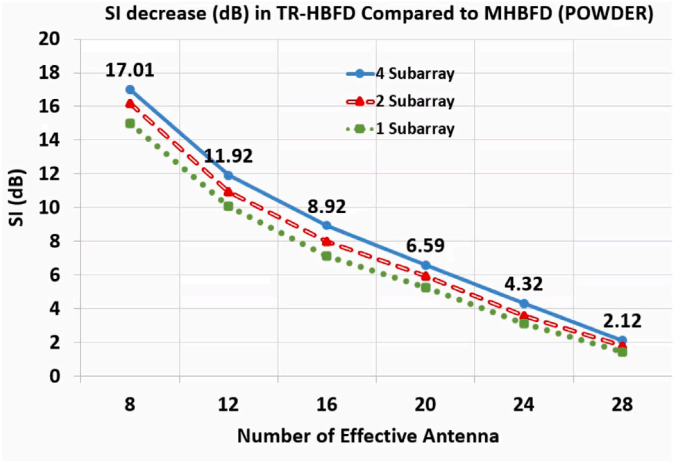

(a) POWDER setup.

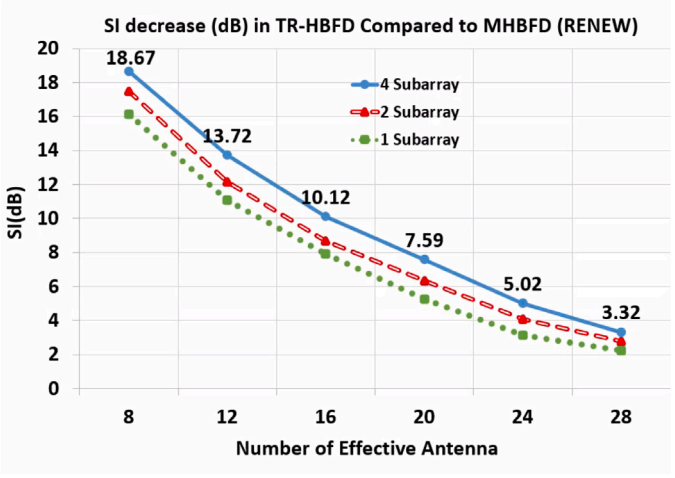

(b) RENEW setup

Fig. 7. POWDER and RENEW SI results for M-HBFD and TR-HBFD. Both systems rely on a hybrid beamforming radio architecture. TR-HBFD uses both transmit and receive antennas to reduce SI, which suppresses interference more than just using Tx beamforming only.

beamforming only for SI suppression in hybrid beamforming systems. Fig. 7 illustrates the influence of the number of subarrays and effective antennas on SI reduction, comparing TR-HBFD and M-HBFD across the two testbeds. The x-axis represents the number of effective antennas, while the y-axis indicates the level of SI reduction in decibels (dB). Overall, TR-HBFD demonstrates superior SI cancellation compared to M-HBFD. This is because some receive antennas are being used to reduce SI in addition to Tx antennas. However, as the number of effective antennas increases, TR-HBFD's advantage diminishes relative to M-HBFD. In the best case scenario, TR-HBFD achieves nearly 19 dB more of SI reduction compared to M-HBFD with four subarrays on the RENEW platform.

5.3. System capacity

Tx Beamforming Only. Fig. 8 illustrates the impact of the number of subarrays and effective antennas on the total sum capacity (uplink + downlink) for Tx beamforming using SoftNull and M-HBFD on the POWDER testbed. Each data point represents the average of 1000 channel realizations. The average Received Signal Reference Power (RSRP) levels for UL and DL transmissions are presented in Tables 3 and 4, respectively.

We observe that M-HBFD has a lower DL RSRP than SoftNull, which is due to the restriction in its beamforming capability as M-HBFD uses a hybrid beamforming radio. Further, another contributing factor is the differences in beamforming gain resulting from different beamforming methods used in SoftNull and M-HBFD. The SoftNull precoder selects D_{Tx} effective antennas that minimize interference on the receive array by performing SVD on the self-interference matrix (denoted by $\mathbf{H}_{\text{self}}$) between all transmit and receive antennas, and sets the remaining highly correlated antennas ($M_{Tx} - D_{Tx}$), which contribute the most to self-interference,

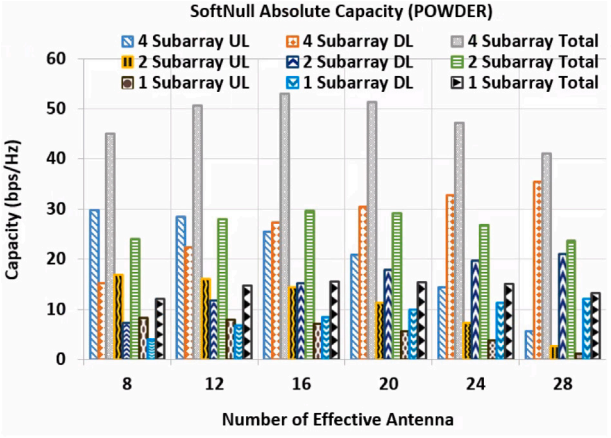

(a) POWDER setup.

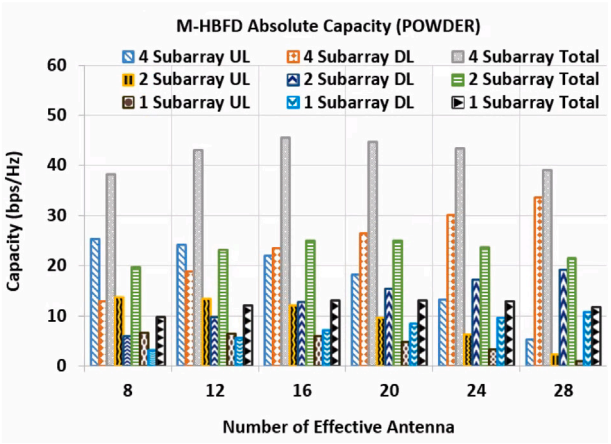

(b) RENEW setup

Fig. 8. POWDER absolute capacity results for Tx beamforming only comparing SoftNull and M-HBFD.

Table 3
Average RSRP levels of UL (dBm), measured across users for different numbers of effective antennas on the POWDER platform.

Algorithm	Eff-Ant = 28	Eff-Ant = 24	Eff-Ant = 20	Eff-Ant = 16	Eff-Ant = 12	Eff-Ant = 8
SoftNull - 4 Subarrays	−74	−70.4	−68.61	−70.79	−74.9	−79.8
M-HBFD - 4 Subarrays	−75.3	−73.4	−74.23	−79.27	−87.1	−95
SoftNull - 2 Subarrays	−74.62	−70.38	−67.41	−68.07	−72.06	−77.01
M-HBFD - 2 Subarrays	−78.74	−76.33	−75.74	−79.24	−86.81	−95.67
SoftNull - 1 Subarrays	−75.43	−69.68	−67.49	−68.42	−72.44	−77.53
M-HBFD - 1 Subarrays	−80.71	−77.8	−78	−82.29	−91.28	−100.87

Table 4
Average RSRP levels of DL (dBm), measured across users for different numbers of effective antennas on the POWDER platform.

Algorithm	Eff-Ant = 28	Eff-Ant = 24	Eff-Ant = 20	Eff-Ant = 16	Eff-Ant = 12	Eff-Ant = 8
SoftNull - 4 Subarrays	−13.33	−15.33	−17.09	−19.41	−23.33	−28.91
M-HBFD - 4 Subarrays	−14.68	−17.31	−20.1	−22.34	−25.92	−30.79
SoftNull - 2 Subarrays	−8.24	−10.44	−13.05	−17.11	−22.31	−29.48
M-HBFD - 2 Subarrays	−11.10	−14.01	−16.84	−20.81	−25.41	−31.68
SoftNull - 1 Subarrays	−3.57	−6.34	−10.26	−14.57	−19.56	−28.49
M-HBFD - 1 Subarrays	−7.61	−11.07	−14.75	−18.68	−23.32	−31.10

to zero. In contrast, M-HBFD divides the transmit array into N_{Tx} subarrays and performs SVD on the self-interference matrix (denoted by $\mathbf{H}_{\text{sub}_{i,\text{all}}}$) for each subarray. Thus, the selection of effective antennas differs between the two methods, leading to different beamforming gains and RSRP levels.

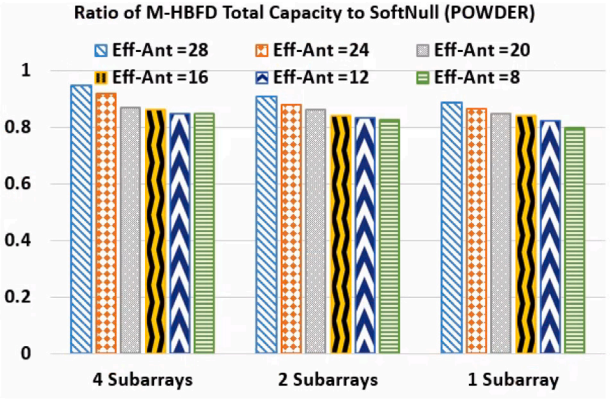

(a) POWDER setup.

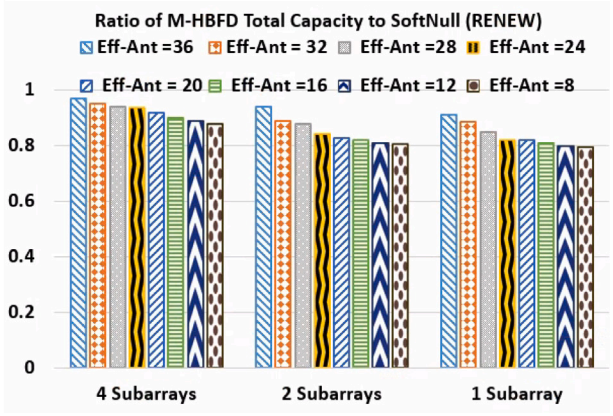

(b) RENEW setup

Fig. 9. POWDER and RENEW capacity results for Tx beamforming only. The total capacity of M-HBFD is within about 20% of SoftNull. In the best case, the total sum capacity of M-HBFD can reach up to 97% of Softnull.

UL and DL achievable capacity rates are computed as follows [15]: For each channel realization p, we calculate the signal-to-interference-plus-noise ratio (SINR) for each DL user j, denoted as $SINR_d(p, j)$. To determine the average ergodic achievable DL capacity, we sum the SINR values across all DL users and then average this sum over all channel realizations as follows:

$$C_d = \frac{1}{N_p} \sum_{P=1}^{N_P} \sum_{j=1}^{K_d} \log_2[1 + SINR_d(p, j)] \tag{8}$$

where N_p is the number of channel realizations. Similarly, for the UL, the average ergodic achievable capacity is obtained by summing the capacities over all UL users and averaging these sums over the channel realizations as follows:

$$C_u = \frac{1}{N_p} \sum_{P=1}^{N_P} \sum_{j=1}^{K_u} \log_2[1 + SINR_u(p, j)]. \tag{9}$$

Fig. 9 illustrates the impact of the number of subarrays and effective antennas on the total M-HBFD sum capacity in comparison to SoftNull on both POWDER and RENEW setups. In both testbeds, the total capacity of M-HBFD was found to be within about 20% of the SoftNull. In the best case, the total sum capacity of M-HBFD can reach up to 95% and 97% of the SoftNull on POWDER and RENEW setups, respectively. We also observe that with the increase in the number of effective antennas, the gap between the two systems shrinks. Effective antennas capture the number of antennas used for DL communication. As the number of effective antennas increase, there is less resource for SI cancellation. This shrinks the gap between the two systems in terms of SI (as depicted in Fig. 5) as well as the gap in DL beamforming, which together manifests itself in shrinking gaps in terms of total capacity.

Joint Tx-Rx Beamforming. Fig. 10 illustrates the impact of the number of subarrays and effective antennas on the total sum capacity of TR-HBFD compared to TR-FD^2. Across both testbeds, the total capacity of TR-HBFD was found to be approximately within 20% of that achieved by TR-FD^2. In the best case, the total sum capacity of TR-HBFD can reach up to 98% and 99% of SoftNull on

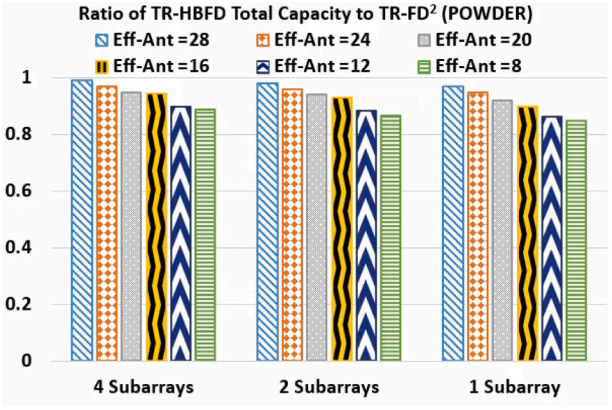

(a) POWDER setup.

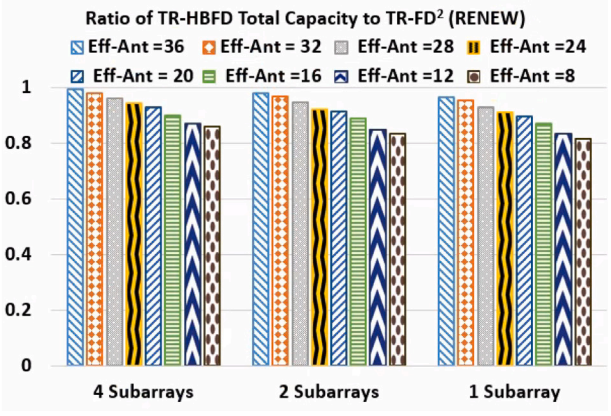

(b) RENEW setup

Fig. 10. POWDER and RENEW capacity results for joint Tx-Rx beamforming. The gap in overall capacity between fully digital and hybrid beamforming shrinks when joint beamforming is employed.

POWDER and RENEW setups, respectively. We observe a consistent trend, akin to Tx beamforming only, with an increase in the number of effective antennas. However, there is an overall performance improvement due to the narrower performance gap in SI cancellation, as depicted in Fig. 6, compared to Tx beamforming only.

Comparison Between Tx Only and Joint Tx-Rx Beamforming. In the previous results, we compared each hybrid beamforming architecture against the corresponding fully digital architecture counterpart. We next, compare the change in capacity between M-HBFD and TR-HBFD. Note that both of these radio architectures assume hybrid beamforming. Fig. 11 shows the ratio of M-HBFD capacity total capacity to TR-HBFD across the two testbeds. We observe that M-HBFD achieves 70%–96% of TR-HBFD capacity depending on the number of effective antennas. TR-HBFD uses its antennas to simultaneously increase UL user signal strength and reduce SI, which in turns increases its capacity.

5.4. Capacity per RF chain

Tx Beamforming Only. Fig. 12 shows the impact of the number of subarrays and effective antennas on the total sum capacity per RF chain. Per RF chain capacity can also be considered as a cost saving metric. The error bar on each data point represents the variation of the capacity for different numbers of effective antennas. Results indicate that M-HBFD consistently outperforms SoftNull by a factor of at least 7 and 9 on POWDER and RENEW testbeds, respectively, and in the best case, it has 27× and 33× higher capacity with only one RF chain.

The results show that the proposed hybrid architecture and the associated SI cancellation method for mMIMO systems is more advantageous than the fully digital architecture as it deploys far fewer RF chains. Note that in M-HBFD, as the number of users increases, the required number of RF chains increases. In one extreme, if the total number of simultaneously served users is equal to the number of antennas, the gap between the two disappears. However, in practical mMIMO systems it is expected that the number of simultaneously served users to be far smaller than the number of antennas. Thus, we expect in practical deployments, hybrid systems to provide comparable performance to fully digital systems in terms of SI and capacity at a fraction of the cost.

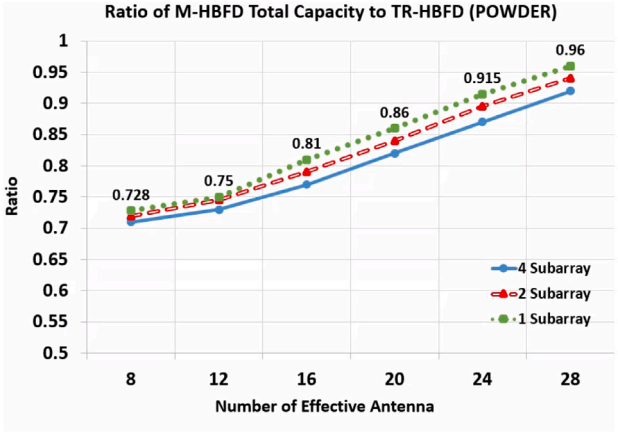

(a) POWDER setup.

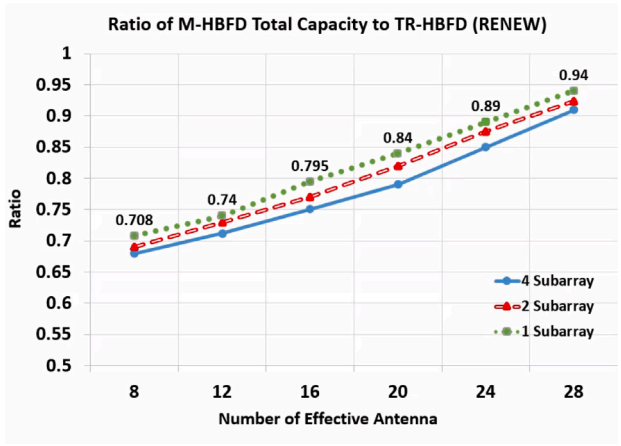

(b) RENEW setup

Fig. 11. POWDER and RENEW capacity results for M-HBFD and TR-HBFD. M-HBFD achieves 70%–96% of TR-HBFD capacity depending on the number of effective antennas.

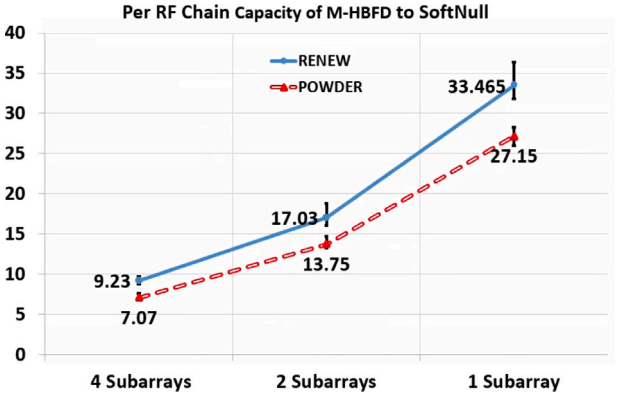

Fig. 12. Per RF chain capacity of M-HBFD to SoftNull as a function of number of subarrays. Error bars capture the varying number of effective antennas.

Joint Tx-Rx Beamforming. Fig. 13 illustrates how the number of subarrays and effective antennas affect the total sum capacity per RF chain for joint Tx-Rx beamforming. The results show that TR-HBFD consistently outperforms SoftNull across both the POWDER and RENEW testbeds. Specifically, TR-HBFD demonstrates a minimum 7-fold and 9-fold improvement over SoftNull on the POWDER and RENEW testbeds, respectively. In the most favorable scenario, TR-HBFD achieves an astounding 29 times and 35

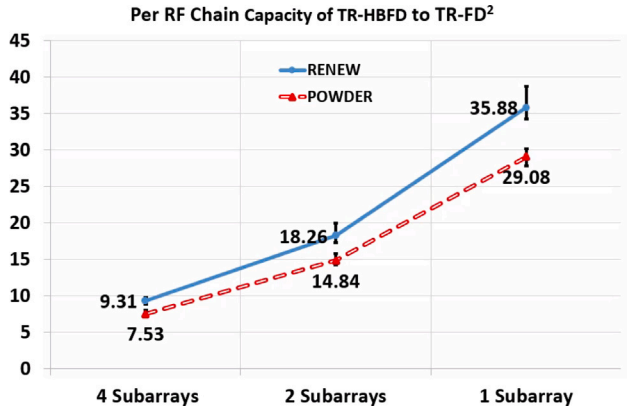

Fig. 13. Per RF chain capacity of TR-HBFD to TR-FD^2 as a function of number of subarrays. Per-RF chain capacity gain with joint beamforming is higher than transmit beamforming only.

times higher capacity with only one RF chain compared to SoftNull. We notice that the total sum capacity per RF chain is higher for joint Tx-Rx beamforming compared to transmit-only beamforming.

6. Conclusion

In this paper, we carried out experiments on two many antenna testbeds. We measured the CSI in three different scenarios including internal measurements on the base station antennas, DL, and UL channels. We then compared the performance of M-HBFD (optimized for hybrid radios) and SoftNull (optimized for fully digital radios). Both methods use transmit beamforming to simultaneously reduce SI and increase the DL beamforming gain. Subsequently, we compared the performance of TR-FD^2 (fully digital architecture for joint Tx-Rx beamforming) with TR-HBFD (hybrid architecture for joint Tx-Rx beamforming). Our study demonstrated that the hybrid beamforming approach achieves similar SI cancellation and capacity rates as the state-of-the-art fully digital solution, even though it uses fewer RF chains. Furthermore, the hybrid beamforming architecture significantly outperforms fully digital algorithms in terms of performance per RF chain. Finally, we showed that the gap in performance (in terms of SI cancellation and capacity) shrinks when joint Tx-Rx beamforming is used as compared to Tx beamforming only.

CRediT authorship contribution statement

Hadi Hosseini: Writing – original draft, Visualization, Validation, Software, Methodology, Formal analysis. **Ahmed Almutairi:** Writing – review & editing, Software, Methodology, Investigation, Data curation. **Syed Muhammad Hashir:** Writing – review & editing, Methodology, Conceptualization. **Ehsan Aryafar:** Writing – review & editing, Project administration, Methodology, Funding acquisition, Formal analysis, Conceptualization. **Joseph Camp:** Writing – review & editing, Supervision, Project administration, Methodology, Funding acquisition, Conceptualization.

Declaration of competing interest

The authors declare that they have no known competing financial interests or personal relationships that could have appeared to influence the work reported in this paper.

Acknowledgments

This research was supported in part by National Science Foundation, USA Grants CNS-1910517, CNS-1942305 and CNS-1909381. We would like to thank Oscar Bejerano and Rahman Doost-Mohammady for their continued support of our measurement campaign, code debugging, and numerous discussions.

References

[1] Cisco VNI: https://blogs.cisco.com/tag/cisco-vni.
[2] A. Sabharwal, P. Schniter, D. Guo, D.W. Bliss, S. Rangarajan, R. Wichman, In-band full-duplex wireless: Challenges and opportunities, in: IEEE Journal on Selected Areas in Communications, 2014.
[3] M. Duarte, A. Sabharwal, Full-duplex wireless communications using off-the-shelf radios: Feasibility and first results, in: Proceedings of IEEE Asilomar, 2010.
[4] M. Duarte, C. Dick, A. Sabharwal, Experiment-driven characterization of full-duplex wireless systems, in: IEEE Transactions on Wireless Communications, 2012.

[5] M. Jain, J. Choi, T. Kim, D. Bharadia, S.S.K. Srinivasan, P. Levis, S. Katti, P. Sinha, Practical, real-time, full duplex wireless, in: Proceedings of ACM MOBICOM, 2011.
[6] D. Bharadia, E. McMilin, S. Katti, Full duplex radios, in: Proceedings of ACM SIGCOMM, 2013.
[7] E. Aryafar, A. Keshavarz-Haddad, FD2: A Directional Full Duplex Communication System for Indoor Wireless Networks, in: Proceedings of IEEE INFOCOM, 2015.
[8] E. Aryafar, M.A. Khojastepour, K. Sundaresan, S. Rangarajan, M. Chiang, MIDU: Enabling MIMO Full Duplex, in: Proceedings of ACM MOBICOM, 2012.
[9] E. Aryafar, A. Keshavarz-Haddad, PAFD: Phased Array Full-Duplex, in: Proceedings of IEEE INFOCOM, 2018.
[10] Y. Kim, H.J. Moon, H. Yoo, B. Kim, K.K. Wong, C.B. Chae, A state-of-the-art survey on full-duplex network design, in: Proceedings of the IEEE, 2024.
[11] B. Smida, A. Sabharwal, G. Fodor, G.C. Alexandropoulos, H.A. Suraweera, C.B. Chae, Full-duplex wireless for 6G: Progress brings new opportunities and challenges, in: IEEE Journal on Selected Areas in Communications, 2023.
[12] R. Chataut, R. Akl, Massive MIMO systems for 5G and beyond networks—overview, recent trends, challenges, and future research direction, in: MDPI Sensors Journal, 2020.
[13] L. Lu, G.Y. Li, A.L. Swindlehurst, A. Ashikhmin, R. Zhang, An overview of massive MIMO: Benefits and challenges, in: IEEE Journal of Selected Topics in Signal Processing, 2014.
[14] A. Shojaeifard, K.K. Wong, M. Di Renzo, G. Zheng, K.H. Hamdi, J. Tang, Massive MIMO-enabled full-duplex cellular networks, in: IEEE Transactions on Communications, 2017.
[15] E. Everett, C. Shepard, L. Zhong, A. Sabharwal, SoftNull: Many-antenna full-duplex wireless via digital beamforming, in: IEEE Transactions on Wireless Communications, 2016.
[16] T. Le-Ngoc, Y. Gong, M. Mahmood, A. Koc, R. Morawski, J.G. Griffiths, P. Guillemette, J. Zaid, P. Wang, Full-duplex in massive multiple-input multiple-output, in: IEEE Open Journal of Vehicular Technology, 2024.
[17] C.K. Sheemar, C.K. Thomas, D. Slock, Practical hybrid beamforming for millimeter wave massive MIMO full duplex with limited dynamic range, in: IEEE Open Journal of the Communications Society, 2022.
[18] A. Koc, T. Le-Ngoc, Full-duplex mmwave massive MIMO systems: A joint hybrid precoding/combining and self-interference cancellation design, in: IEEE Open Journal of the Communications Society, 2021.
[19] S. Huang, Y. Ye, M. Xiao, Learning-based hybrid beamforming design for full-duplex millimeter wave systems, in: IEEE Transactions on Cognitive Communications and Networking, 2020.
[20] Y. Cai, K. Xu, A. Liu, M. Zhao, B. Champagne, L. Hanzo, Two-timescale hybrid analog-digital beamforming for mmwave full-duplex MIMO multiple-relay aided systems, in: IEEE Journal on Selected Areas in Communications, 2020.
[21] T. Chen, M.B. Dastjerdi, H. Krishnaswamy, G. Zussman, Wideband full-duplex phased array with joint transmit and receive beamforming: Optimization and rate gains, in: IEEE/ACM Transactions on Networking, 2021.
[22] R. López-Valcarce, M. Martínez-Cotelo, Full-duplex mmwave communication with hybrid precoding and combining, in: Proceedings of the 28th European Signal Processing Conference, EUSIPCO, 2021.
[23] I. Cummings, J. Doane, T. Schulz, T. Havens, Aperture-level simultaneous transmit and receive with digital phased arrays, in: IEEE Transactions on Signal Processing, 2020.
[24] N. Gowda, A. Sabharwal, JointNull: Combining partial analog cancellation with transmit beamforming for large-antenna full-duplex wireless systems, in: IEEE Transactions on Wireless Communication, 2018.
[25] POWDER: https://powderwireless.net/.
[26] RENEW website: https://renew.rice.edu/.
[27] G. Megson, S. Gupta, S. Hashir, E. Aryafar, J. Camp, An experiment-based comparison between fully digital and hybrid beamforming radio architectures for many-antenna full-duplex wireless communication, in: MDPI Electronics Journal, 2021.
[28] H. Hosseini, A. Almutairi, S.M. Hashir, E. Aryafar, J. Camp, An outdoor experimental study of many antenna full-duplex wireless, in: International Teletraffic Congress, 2023.
[29] Code Repository: https://guanyin.cs.pdx.edu/repository.html.
[30] R. Sultan, K.G. Seddik, Z. Han, B. Aazhang, Joint transmitter-receiver optimization and self-interference suppression in full-duplex MIMO systems, in: IEEE Transactions on Vehicular Technology, 2021.
[31] G. Wang, Z. Yang, T. Gong, C. Xie, Self-interference cancellation based hybrid beamforming design for full-duplex mmwave communication with partially-connected structures, in: Proceedings of IEEE ICCT, 2020.
[32] R. López-Valcarce, N. González-Prelcic, Analog beamforming for full-duplex millimeter wave communication, in: Proceedings of the 16th International Symposium on Wireless Communication Systems, ISWCS, 2019.
[33] G. Alexandropoulos, M. Islam, B. Smida, Full duplex hybrid a/d beamforming with reduced complexity multi-tap analog cancellation, in: Proceedings of the IEEE 21st International Workshop on Signal Processing Advances in Wireless Communications, SPAWC, 2020.
[34] Y. Cao, J. Zhou, Integrated self-adaptive and power-scalable wideband interference cancellation for full-duplex MIMO wireless, in: IEEE Journal of Solid-State Circuits, 2020.
[35] L. Ordoñez, P. Ferrand, M. Duarte, M. Guillaud, G. Yang, On full-duplex radios with modulo-ADCs, in: IEEE Open Journal of the Communications Society, 2021.
[36] G. Wang, Z. Yang, T. Gong, Hybrid beamforming design for self-interference cancellation in full-duplex millimeter-wave MIMO systems with dynamic subarrays, in: MDPI Entropy Journal, 2022.
[37] M. Mahmood, A. Koc, R. Morawski, T. Le-Ngoc, Achieving capacity gains in practical full-duplex massive mimo systems: A multi-objective optimization approach using hybrid beamforming, in: IEEE Open Journal of the Communications Society, 2024.
[38] RENEW Code: https://github.com/renew-wireless/RENEWLab.git.